Hendrik Vennekate, Christian Reichardt, Arne Walter,
Harald Fuest, Jörg Schroeder*, and Dirk Schwarzer

# Femtosecond Infrared Spectroscopy of Aroylperoxide Photofragmentation – Site Selective Decarboxylation

DOI 10.1515/zpch-2015-0629
Received April 17, 2015; accepted June 7, 2015

**Abstract:** The ultrafast photofragmentation of acetyl-benzoyl peroxide (ABPO) and 2-naphthoyl-benzoyl peroxide (NBPO) after UV excitation at 266 nm is studied by mid-infrared transient absorption spectroscopy. $^{13}$C-isotopic labelling is employed to unravel the primary fragmentation paths. For NBPO it appears that excitation of the benzoyloxy part causes decarboxylation exclusively at that site. In ABPO the acetyloxy part completely decarboxylates upon 266 nm excitation while only 80%–85% of the benzoyloxyl radicals formed decarboxylate. The remaining radicals either combine with methyl radicals to methylbenzoate within about 30 ps or survive on the time scale of the experiment (1.5 ns). Photofragmentation of ABPO occurs from the $S_1$-state whose lifetime is about 200 fs. All fragmentation products including $CO_2$ also appear on this time scale.

**Keywords:** Reaction Dynamics, Photochemistry, Femtosecond IR Spectroscopy.

**Dedicated to** Prof. Dr. Dr. h.c. mult. Jürgen Troe on the occasion of his 75$^{th}$ birthday

## 1 Introduction

Organic peroxides form a group of molecules for which a thorough understanding of reactivity on an ultra-short time-scale is of both fundamental and technical interest. Photochemical or thermal decomposition of these substances yields radicals that are widely employed to initiate macromolecular growth in free-radical

***Corresponding author: Jörg Schroeder,** Max-Planck-Institut für Biophysikalische Chemie, Am Fassberg 11, 37070 Göttingen, Germany, e-mail: jschroe2@gwdg.de
**Hendrik Vennekate, Christian Reichardt, Arne Walter, Harald Fuest, Dirk Schwarzer:** Max-Planck-Institut für Biophysikalische Chemie, Am Fassberg 11, 37070 Göttingen, Germany

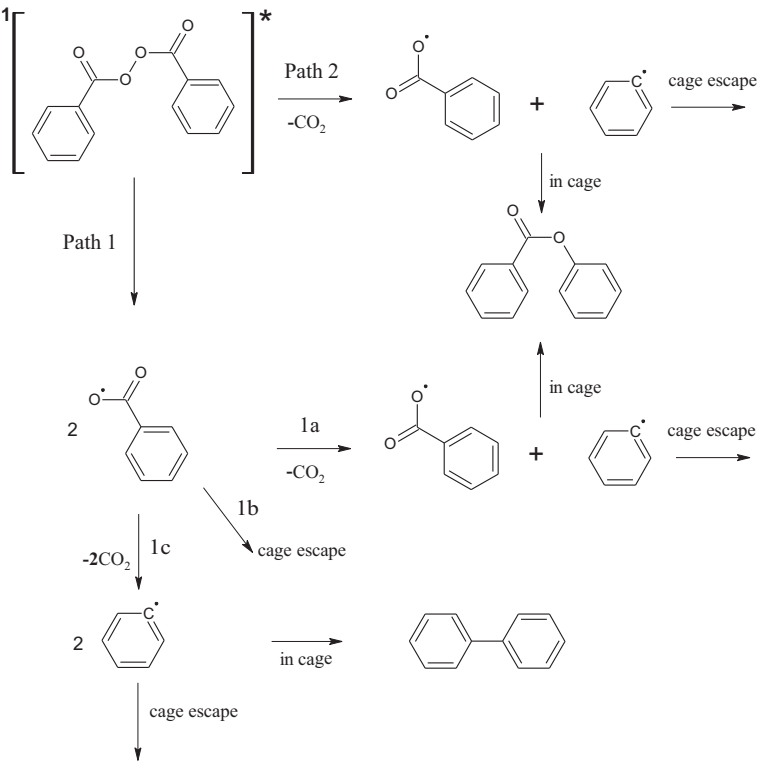


**Figure 1:** Suggested decarboxylation mechanisms of singlet excited dibenzoyl peroxide (DBPO).

polymerization. Successful initiation encompasses several elementary kinetic steps from the primary dissociation event of the parent peroxide molecule to the final addition of a peroxide-derived free-radical species to a monomer molecule. The kinetic scheme in Figure 1 illustrates the early stages of this reaction sequence for dibenzoyl peroxide (DBPO), a well-studied representative of this class of compounds. Initiator efficiency depends on the type of radicals produced in the primary step and on their escape probability from the solvent cage. Fast decarboxylation of the intermediate carbonyloxy radical lowers initiator efficiency and may affect polymer properties, as carbon-centered radicals have significantly lower chain-transfer than the oxygen-centered radicals. It is therefore essential to understand the dynamics of the elementary steps following initial O–O bond scission.

The thermal decomposition of DBPO is known to proceed via breakage of the O–O bond yielding two benzoyloxyl radicals (path 1) which escape the solvent cage (path 1b) and subsequently either decarboxylate on a microsecond time

scale to form phenyl radicals or react, e.g., with the solvent or appropriate scavengers [1]. The primary steps of UV photo-induced fragmentation of DBPO, on the other hand, had remained unclear until recently. Early chemical trapping experiments [2] showed that UV-photolysis not only yields benzoyloxyl radicals (which later were characterized by their UV-VIS [3] and EPR [4, 5] spectra), but by two bond cleavage also phenyl radicals and $CO_2$ as well as phenyl benzoate formed by geminate recombination of the benzoyloxyl-phenyl radical pair in the solvent cage [6]. Consistent with this interpretation is the observation that all $CO_2$ is formed within 10 ps after excitation [7], suggesting that decarboxylation involves either rapid sequential bond scission starting along path 1 and continuing along path 1a/1c or a concerted two-bond cleavage (path 2).

Recent femtosecond pump-probe experiments employing 267 nm excitation [8] seemed to favor a rapid sequential mechanism. The authors assigned observed picosecond transients in the visible to near-IR spectral range to hot benzoyloxyl radicals, and suggested that DBPO photofragmentation initially follows path 1 with O–O-bond scission being faster than 200 fs, yielding a distribution of vibrationally excited benzoyloxyl radicals. The highly excited fraction of these then decomposes rapidly to phenyl plus $CO_2$ (path 1a), while the remaining benzoyloxyl radicals vibrationally relax on a picosecond timescale to thermal equilibrium and escape the solvent cage (path 1b).

This interpretation, however, rests upon the correct assignment of transient electronic spectra in the visible and near IR. Vibrational absorption bands, on the other hand, are much narrower than electronic spectra and characteristically depend on details of molecular structure, such that femtosecond broadband IR spectroscopy can provide additional information on the mechanism of complex photoreactions. Using femtosecond UV excitation at 266 nm and mid-infrared broadband detection, we have recently been able to elucidate more details of DBPO photofragmentation [9, 10]. We could show that the $S_1$-lifetime of the photo excited DBPO molecule in solution is extremely short ($0.4 \pm 0.2$ ps) and that vibrationally hot $CO_2$ molecules as well as benzoyloxyl radicals are formed at the same rate as the $S_1$-state absorption decays. After this initial fragmentation, the $CO_2$ concentration does not increase further during the observation time of 1 ns, and we determined a quantum yield of $\Phi_{CO_2} = 1.0$. The benzoyloxyl radical concentration decreases by 15%–25% with a time constant of $(70 \pm 10)$ ps, exactly matching the formation rate of the geminate recombination product phenyl benzoate. Consequently, DBPO photodecarboxylation follows the mechanism depicted in Figure 2.

Though we succeeded in clarifying the fragmentation mechanism down to a timescale of about half a picosecond, the underlying dynamics remain unknown. So far we have no measurements that would allow us to distinguish be-

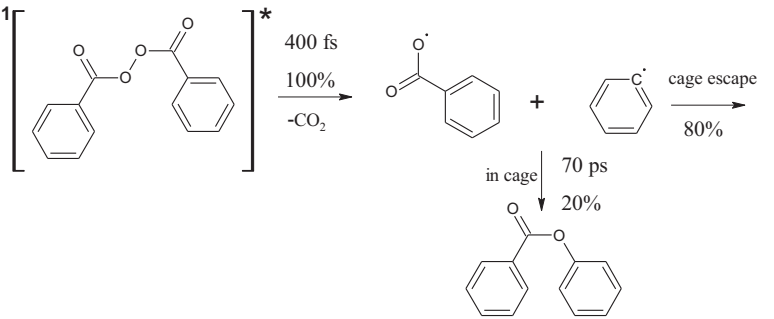


**Figure 2:** Timescales and yields of DBPO photofragmentation.

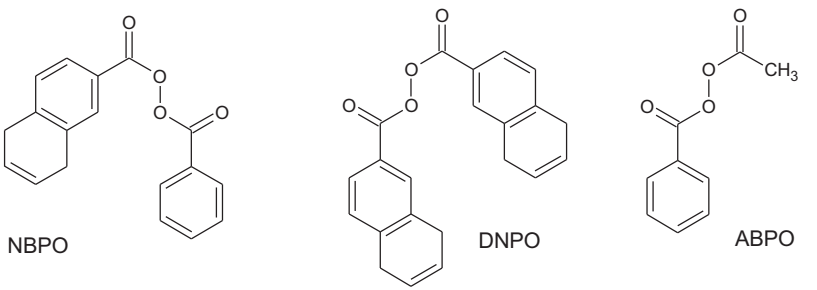


**Figure 3:** Structures of aroylperoxides used in this study.

tween concerted O–O-/C–C-bond scission and ultrafast sequential breakage of first the O–O-bond and then the C–C-bond to produce $CO_2$ on this timescale. In this context it would be helpful to know if, under conditions of single photon excitation of DBPO where one of the two benzoyloxyl chromophores absorbs the photon, the C–C-bond closer to the initially excited chromophore breaks preferentially or whether the energy delocalizes across the molecule before one of the two $CO_2$ molecules is eliminated.

An early claim of an observation of corresponding photoselectivity in crystalline DBPO [11] was later shown to be associated with crystal anisotropy rather than selective excitation of DBPO [12]. This already demonstrated that it is difficult to find an answer to this question by studying the symmetric molecule DBPO, as in solution we cannot devise a method to selectively excite a specific chromophore. Instead, we address this question by investigating the quite similar asymmetric molecule 2-naphthoylbenzoyl-peroxide (NBPO) and, for comparison, acetylbenzoylperoxide (ABPO) (chemical structures are given in Figure 3).

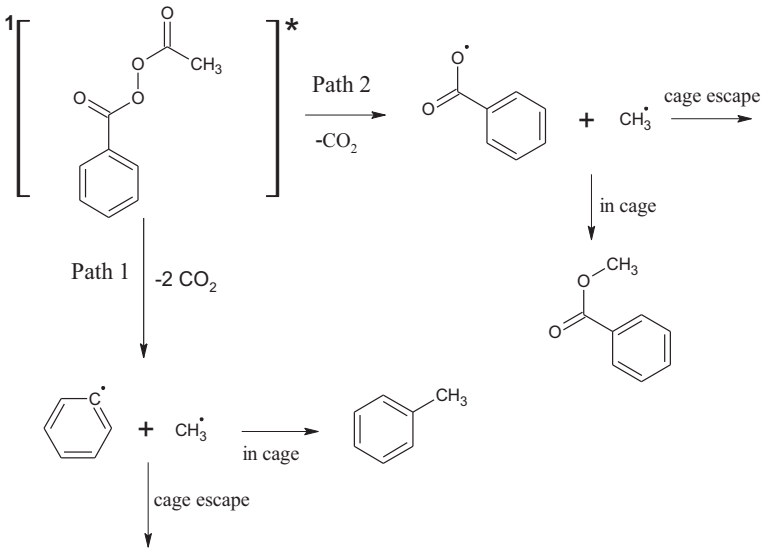


**Figure 4:** Photofragmentation mechanism of ABPO [14–16].

NBPO is an obvious candidate for this study, because DBPO and the related compound di-(2-naphthoyl)peroxide (DNPO), where both benzoyl groups are replaced by naphthoyl, show quite similar decarboxylation characteristics.

In particular, following UV-excitation at 266 nm of DNPO, its $S_1$-absorption decays with a time constant of 0.4 ps [13], while after excitation at 310 nm the IR-absorption of the $CO_2$ asymmetric stretch reaches its maximum within the experimental time resolution of a few picoseconds [7]. Further evidence for this similarity is provided by transient IR-measurements on DNPO presented in this study. Our results on DBPO and DNPO seem to justify the assumption that the kinetics of NBPO photodecarboxylation at the naphthoyloxyl and the benzoyloxyl site are equivalent.

This assumption, of course, is not valid for ABPO, as decarboxylation of the acetoxyl radical is much more facile than of the benzoyloxyl radical. In addition to $CO_2$, the primary products of ABPO photofragmentation are methyl, benzoyloxyl and phenyl radicals, whereas no evidence for acetoxyl radicals has been found [14, 15]. Conceivable reaction paths are summarized in Figure 4.

## 2 Experimental

Femtosecond UV pump/IR probe experiments were carried out with a laser system based on a 1 kHz Ti:sapphire chirped-pulse regenerative amplifier system [17] delivering 100 fs pulses with energies of 700 μJ. Part of the 800 nm light was used to produce pump pulses at 267 nm by frequency tripling. Tunable mid-IR probe pulses were generated by difference frequency mixing of idler and signal from an optical parametric amplifier [18, 19] pumped by 250 μJ pulse energy of the regenerative amplifier output. The UV light was attenuated to energies of 0.5–2 μJ and used to excite 1.5–4 mM solutions of ABPO dissolved in $CD_3CN$ (Deutero GmbH, 99.6% deuteration grade) or $CCl_4$. The IR light was split in a probe and a reference beam and focused into the sample cell. At the sample the probe pulse was superimposed on the pump beam. To avoid signal contributions arising from rotational relaxation of molecules the relative plane of polarization of both pulses was adjusted to 54.7°. After passing the cell both IR beams were spectrally dispersed in a grating polychromator and independently imaged onto a HgCdTe detector (2 × 32 elements). The whole pump-probe setup was purged with dry nitrogen to avoid spectral and temporal distortion of the IR pulses by $CO_2$ and water absorptions in air. All experiments were performed in a stainless steel flow cell equipped with 1 mm thick $CaF_2$ windows (path length inside the cell 0.6–1.5 mm). To obtain a better match between the stationary and transient IR spectra, the line width of the former was adapted to the resolution of the pump-probe spectrometer of 7 $cm^{-1}$, which is given essentially by the dispersion of the spectrograph and the pixel width of the HgCdTe-detector. Accordingly, the stationary spectra reported here were computed from a convolution of the measured FT-IR spectra with a rectangular function of 7 $cm^{-1}$ width. The band intensities are not affected by this procedure.

In addition, transient spectra in the near UV and visible were measured with a white-light continuum probe pulse. The continuum was generated by focusing 10 μJ of the amplified 800 nm pulse into a $CaF_2$ crystal of 4 mm length and split into a reference and probe pulse. The latter was overlaid with the UV pump pulse at the sample. Each continuum was detected with a 256 element linear diode array attached to a spectrograph. The measured transient spectra were corrected with respect to the group delay dispersion of the probe continuum [20].

To distinguish the two $CO_2$ units we $^{13}$C-labeled either the acetyl or the benzoyl carbonyl group of ABPO to obtain $^{13}$ABPO and A$^{13}$BPO, respectively. Synthesis of these compounds started from benzoic acid ($^{13}$C-benzoic acid) which was transformed into perbenzoic acid ($^{13}$C-perbenzoic acid) [21] and then treated with $^{13}$C-acetyl chloride (acetyl chloride) [22] to yield the desired compounds.

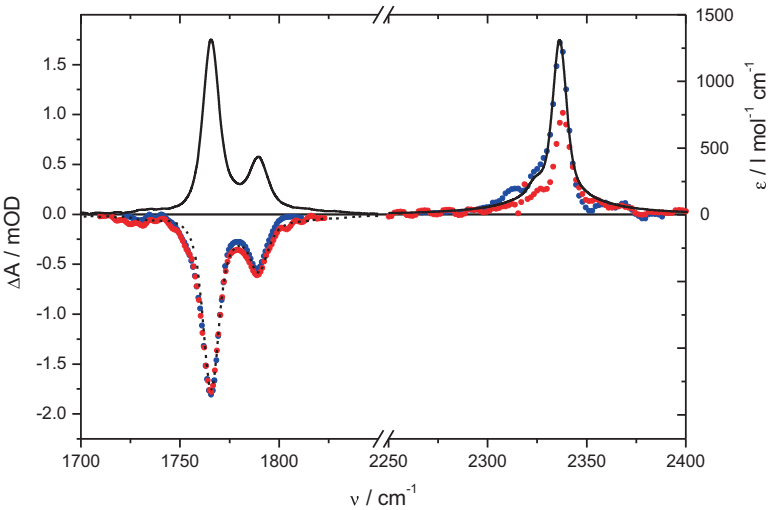


**Figure 5:** IR-absorption bands of DNPO C=O-stretch (1750–1800 cm$^{-1}$) and $CO_2$ asymmetric stretch (2300–2350 cm$^{-1}$) in $CCl_4$. Black solid line/right scale: stationary spectrum. Transient spectra 1.5 ns after UV-excitation (left scale) at 266 nm (blue points) and 300 nm (red points). The dashed black line is the inverted stationary absorption band of the C=O-stretch.

# 3 Results and discussion

## 3.1 DNPO

In order to describe DBPO and DNPO photodecarboxylation quantitatively, we determined the quantum yield of $CO_2$ in the UV-photolysis of DNPO as shown in Figure 5. For that purpose we compared the transient IR absorption and bleach signals observed 1.5 ns after UV-excitation of DNPO (colored points) with the stationary spectra, i.e. the absorption bands of the C=O-stretch (1750–1800 cm$^{-1}$) and the $CO_2$ asymmetric stretch (2300–2350 cm$^{-1}$) (black lines). After matching the transient bleach of the C=O-stretch to the corresponding inverted stationary absorption, we directly obtain the $CO_2$ quantum yield from a comparison of the amplitudes of the transient $CO_2$ asymmetric stretch band and the corresponding stationary band. For 266 nm pump wavelength one finds a perfect match between the two, i.e., $\Phi_{CO_2} = 1.0 \pm 0.1$ for DNPO photolysis at this wavelength, as we found previously for DBPO. When we excite DNPO at 300 nm, the quantum yield decreases to $\Phi_{CO_2} = 0.6 \pm 0.1$. We will compare these results with those of the UV-photolysis of NBPO in the next section.

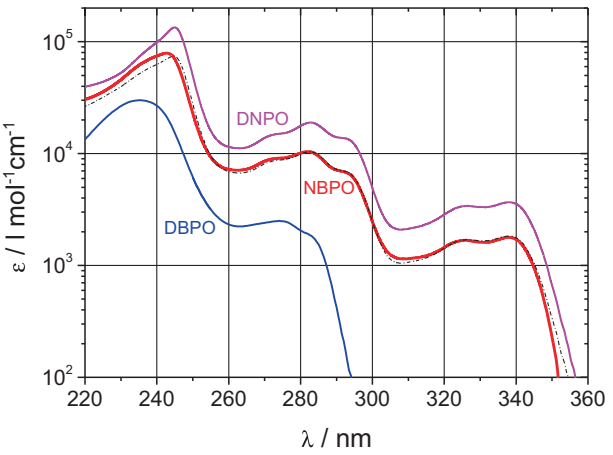


**Figure 6:** Stationary UV-absorption spectra of DPBO (blue), DNPO (magenta), and NBPO (red) in $CH_3CN$. The black dashed line represents the average of the DPBO and DNPO spectra.

## 3.2 NBPO

Before we compare the photodecarboxylation characteristics of DBPO, DNPO and NBPO, we consider the stationary UV-absorption spectra shown in Figure 6. One may note that the spectrum of NBPO is an almost perfect average of the absorption spectra of the symmetric compounds DBPO and DNPO. We therefore may assume that single photon absorption takes place in one of the unperturbed chromophores, either the naphthoyl or the benzoyl group.

Taking this reasoning one step further, we consider that excitation at around 300 nm will initially excite the naphthoyl side, while irradiation at 266 nm will generate NBPO molecules with the excitation initially localized on the naphthoyl or the benzoyl group at a population ratio of almost exactly 5 : 1.

The question we want to address is whether $CO_2$ is eliminated preferentially at the excited site. This requires selective $^{13}C$-labeling of one of the carboxyl groups. We chose the one at the benzoyloxyl group. Figure 7A shows the transient IR-absorption bands of the asymmetric stretch of $^{12}CO_2$ and $^{13}CO_2$ 1.5 ns after excitation of NBPO at 310 nm. Here only the naphthoyl site absorbs, and we find that $CO_2$-elimination at the naphthoyl site seems favored by a factor of 3.2 over that at the benzoyl site, i.e. about 3 out of four excited NBPO molecules eliminate $CO_2$ at the naphthoyl site. When we decrease the excitation wavelength to 266 nm, where both moieties absorb, this factor drops to 2.6. The relative yields of $^{12}CO_2$ and $^{13}CO_2$ do not depend on pump intensity and the signal amplitudes scale linearly with it, indicating single photon excitation. (Figure 7B). Presuming that at 266 nm five out of six absorbed photons primarily excite the naphthoyl

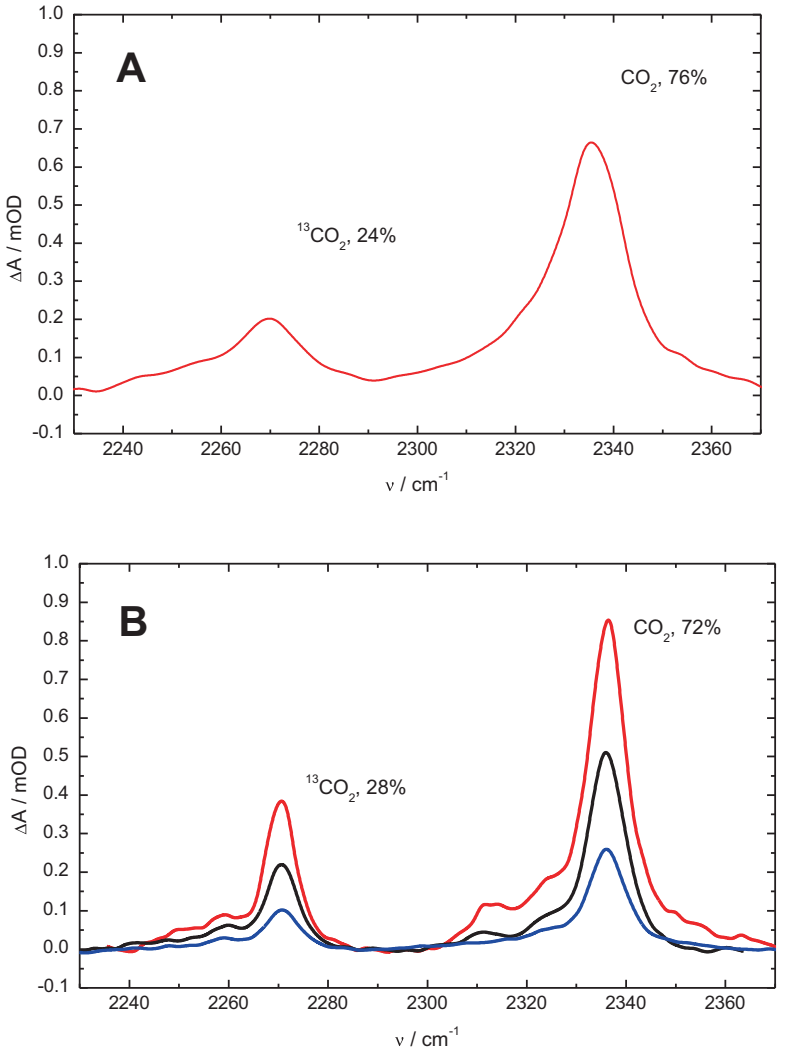


**Figure 7:** Relative yields of $^{12}CO_2$ and $^{13}CO_2$ after UV-photolysis of NBPO. A: Excitation at 310 nm in *n*-heptane solvent. B: Excitation at 266 nm in MeCN solvent with relative pump intensity 0.3 (blue), 0.5 (black), and 1.0 (red).

chromophore, the observed decrease of the relative yield of $^{12}CO_2$ is just what one would get, if every photon that excites the benzoyloxyl moiety leads to $^{13}CO_2$ elimination at that same site.

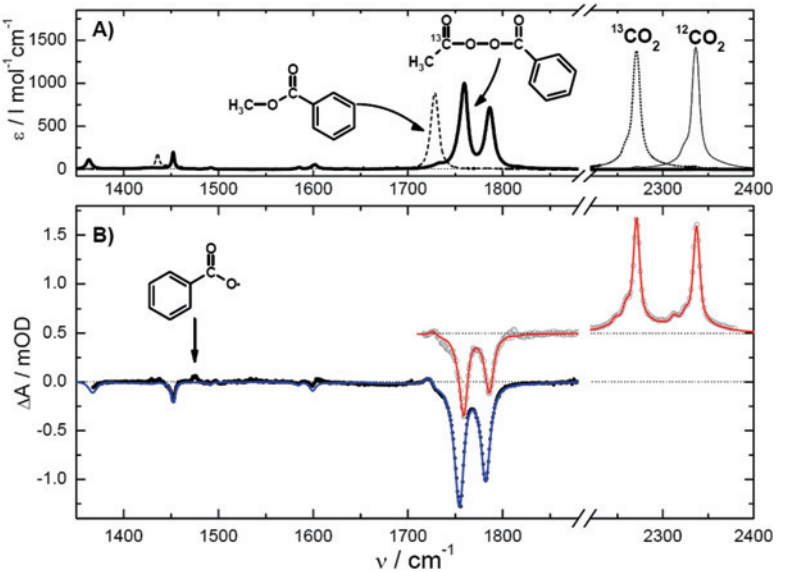


**Figure 8:** (A). Extinction coefficients of $^{13}$ABPO, methylbenzoate, $^{13}CO_2$, and $^{12}CO_2$ dissolved in $CCl_4$. (B). Transient difference spectra 1.5 ns after 267 nm excitation of $^{13}$ABPO in $CD_3CN$ (filled circles) and $CCl_4$ (open circles, for clarity the data are vertically shifted by 0.5 units). Solid lines are calculated difference spectra assuming 100% bleaching of $^{13}$ABPO and, respectively, 6% methylbenzoate formation (blue) and 8% methylbenzoate, 100% $^{13}CO_2$, and 85% $^{12}CO_2$ formation (red). The arrow indicates a peak attributed to the benzoyloxyl radical.

## 3.3 ABPO

Figure 8A shows extinction coefficients $\varepsilon$ determined from Fourier transform (FT) IR spectra of $^{13}$ABPO, methylbenzoate (MB), $^{13}CO_2$, and $^{12}CO_2$ in $CCl_4$, respectively. $^{13}$ABPO shows two strongly IR active C=O stretch bands at 1750 and 1786 $cm^{-1}$. It is well known that the two carbonyl vibrations in $^{13}$ABPO are strongly coupled generating a low frequency asymmetric stretch and a high frequency symmetric stretch mode [23]. The C=O stretch vibration of MB is well separated from these bands and peaks at 1728 $cm^{-1}$. The asymmetric stretch bands of $CO_2$ in $CCl_4$ are at 2271 $cm^{-1}$ for $^{13}CO_2$ and at 2336 $cm^{-1}$ for $^{12}CO_2$.

In Figure 8B transient difference spectra recorded 1.5 ns after UV excitation of $^{13}$ABPO in $CCl_4$ (open circles) and $CD_3CN$ (filled circles) are presented. The measurements in $CCl_4$ cover the frequency range 1700–2400 $cm^{-1}$ and show bleaching of the peroxide as well as formation of large amounts of $^{13}CO_2$ and $^{12}CO_2$, and a minor contribution of MB. At lower frequencies, where $CCl_4$ is opaque, $CD_3CN$ was used as a solvent. Here, apart from bleaching of $^{13}$ABPO and formation of MB

an additional absorption peak at 1476 $cm^{-1}$ appears which we attribute to the benzoyloxyl radical as it coincides with the spectrum of this species known from our photo-fragmentation study on dibenzoyl peroxide [9, 10]. For a quantitative determination of product quantum yields a sum of spectra of Figure 8A was fitted to the transient spectrum measured in $CCl_4$. For the $CO_2$ asymmetric stretch bands calculated spectra were used because at 1.5 ns these molecules turn out not to be at thermal equilibrium [10, 17, 24]. The red line represents the sum

$$0.08\varepsilon(\mathrm{MB}) + 1.00\varepsilon(^{13}\mathrm{CO_2}) + 0.85\varepsilon(^{12}\mathrm{CO_2}) - 1.00\varepsilon(^{13}\mathrm{ABPO})$$

For the difference spectrum in $CD_3CN$ the same procedure was applied using extinction coefficients measured in acetonitrile not shown here. The blue line is a scaled fit with $0.06\varepsilon(\mathrm{MB}) - 1.00\varepsilon(^{13}\mathrm{ABPO})$. The close agreement of both fits with the measured difference spectra suggests that the photolysis of $^{13}$ABPO leads to a complete fragmentation of the acetoxyl unit within 1.5 ns. For the benzoyloxyl unit only 85% decarboxylation is observed. About 6%–8% of the benzoyloxyl radicals geminately recombine with methyl radicals to form methylbenzoate, the remaining 7%–9% survive as free radicals.

Analogous spectra are presented in Figure 9 for the A$^{13}$BPO molecule. Here the strong coupling between the carbonyl stretch vibrations is lifted upon shifting the $^{13}$C label from the acetyl to the benzoyl carbonyl group. Hence, the IR absorptions of A$^{13}$BPO at 1735 and 1811 $cm^{-1}$ in Figure 9A correspond to modes localized at the benzoyl and the acetyl side, respectively. The C=O stretch vibration of $^{13}$C-methybenzoate is red-shifted with respect to the unlabeled compound to 1686 $cm^{1}$.

The transient difference spectrum in Figure 9B measured 1.5 ns after 266 nm excitation of A$^{13}$BPO in $CCl_4$ (open circles) shows formation of a small amount of ester at 1690 $cm^{-1}$ and much larger amounts of $CO_2$. In contrast to Figure 8B, the amplitude ratio of $^{13}CO_2/^{12}CO_2$ is reversed, i.e. this time more $^{12}CO_2$ than $^{13}CO_2$ is produced. The difference spectrum in $CD_3CN$ (filled circles) shows an additional absorption at 1460 $cm^{-1}$. This peak supports our previous assignment to the benzoyloxyl radical since the isotope shift of 16 ± 1 $cm^{-1}$ and its larger amplitude with respect to the transient spectrum of Figure 8B are consistent with previously measured spectra of this radical [10].

The full lines in Figure 9B were calculated from the stationary spectra of Figure 9A. The red line is the scaled sum of

$$0.08\varepsilon(^{13}\mathrm{MB}) + 0.80\varepsilon(^{13}\mathrm{CO_2}) + 1.00\varepsilon(^{12}\mathrm{CO_2}) - 1.00\varepsilon(\mathrm{A}^{13}\mathrm{BPO})$$

and the blue line corresponds to

$$0.07\varepsilon(^{13}\mathrm{MB}) - 1.00\varepsilon(\mathrm{A}^{13}\mathrm{BPO}),$$

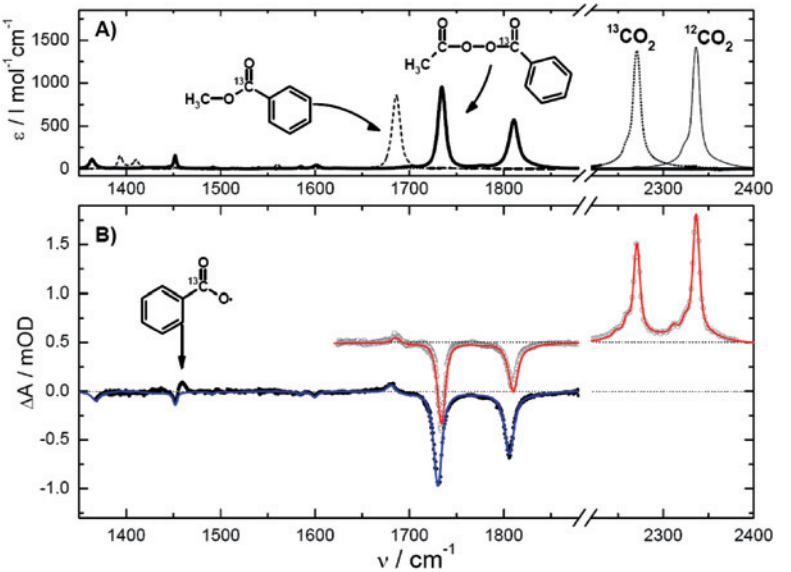


**Figure 9:** (A). Extinction coefficients of A$^{13}$BPO, $^{13}$C-methylbenzoate, $^{13}CO_2$, and $^{12}CO_2$ dissolved in $CCl_4$. (B). Transient difference spectra 1.5 ns after 267 nm excitation of A$^{13}$BPO in $CD_3CN$ (filled circles) and $CCl_4$ (open circles, for clarity the data are vertically shifted by 0.5 units). Solid lines are calculated difference spectra assuming 100% bleaching of A$^{13}$BPO and, respectively, 7% methylbenzoate formation (blue) and 8% methylbenzoate, 80% $^{13}CO_2$, and 100% $^{12}CO_2$ formation (red). The arrow indicates a peak attributed to the $^{13}$C-benzoyloxy radical.

i.e. similar to $^{13}$ABPO, the acetoxyl unit of A$^{13}$BPO is decomposed completely after 1.5 ns. For benzoyloxyl we find 80% fragmentation, 7%–8% recombination to methylbenzoate, and 12%–13% stable radicals.

In the following, we turn to the spectral evolution of the C=O stretch band pair of $^{13}$ABPO in $CD_3CN$ shown in Figure 10. As for previously investigated peroxides [9, 10, 17, 24], after UV excitation we expect to observe a superposition of C=O-band bleach in the $S_0$-state and of a corresponding absorption in the $S_1$-state. In the contour diagram (lower panel) the absorption change is plotted as a function of pump-probe delay and probe wavelength. The upper panel shows a time trace averaged over the probe frequency range 1775–1785 cm$^{-1}$. At positive pump-probe delays a rapid bleaching within the time resolution of our experiment can be observed, while there is no clear evidence of excited state absorption. Up to 1.5 ns no recovery of the bleach component is detected. (The absorbance changes at negative delay times are due to perturbed free induction decay.) Also at other probe frequencies we have no indication of excited state absorption of ABPO. At the same time there is no evidence of delayed formation of benzoyloxyl

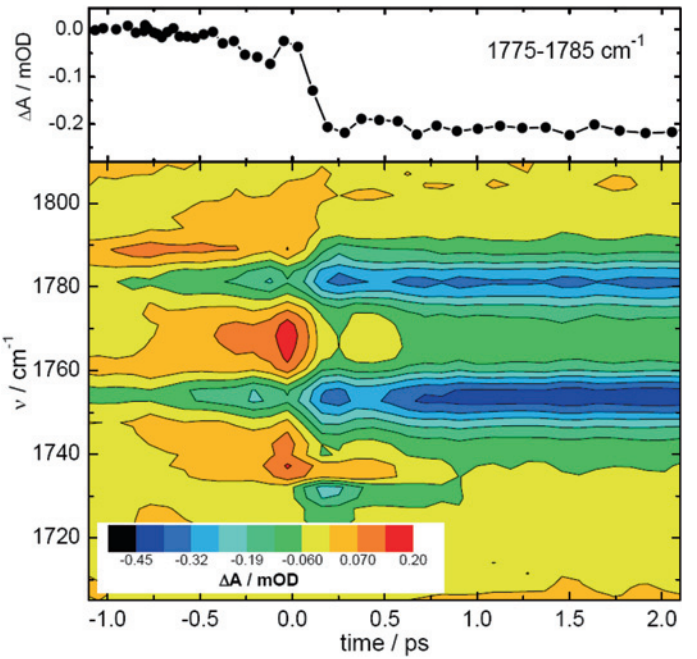


**Figure 10:** Pump-probe difference spectra of the C=O stretching bands of $^{13}$ABPO in $CD_3CN$. The upper panel shows the integrated band intensity in the range 1775–1785 $cm^{-1}$.

and $CO_2$, i.e. all primary fragments are formed within the experimental time resolution. These observations indicate that the lifetime of the excited ABPO molecule must be of the order of 200 fs.

This result is in fair agreement with the ultrafast decay component of the transient UV/VIS absorption following excitation of ABPO in $CH_3CN$ at 258 nm shown in Figure 11. If we integrate over the strong absorption feature between 360 and 400 nm we obtain for the short component a lifetime of 340 fs, which we assign to the $S_1$-state of ABPO. The substantial offset absorption is assigned to the benzoyloxyl radical formed in the photofragmentation. This radical is known to have a prominent absorption band around 390 nm [3, 25].

Figure 12 shows the time evolution of the C=O stretch band of methyl benzoate emerging at 1687 $cm^{-1}$ after UV excitation of A$^{13}$BPO in $CCl_4$. The integral band intensity increases with a characteristic time constant of $\tau = 30 \pm 5$ ps. Initially, the absorption is also shifted to the red and broadened, indicating that the ester is formed vibrationally hot and cools down on a similar timescale as the geminate recombination occurs. The time constant of $\tau = 30$ ps is more than a factor of two shorter than for the geminate recombination of phenyl plus benzoyloxyl

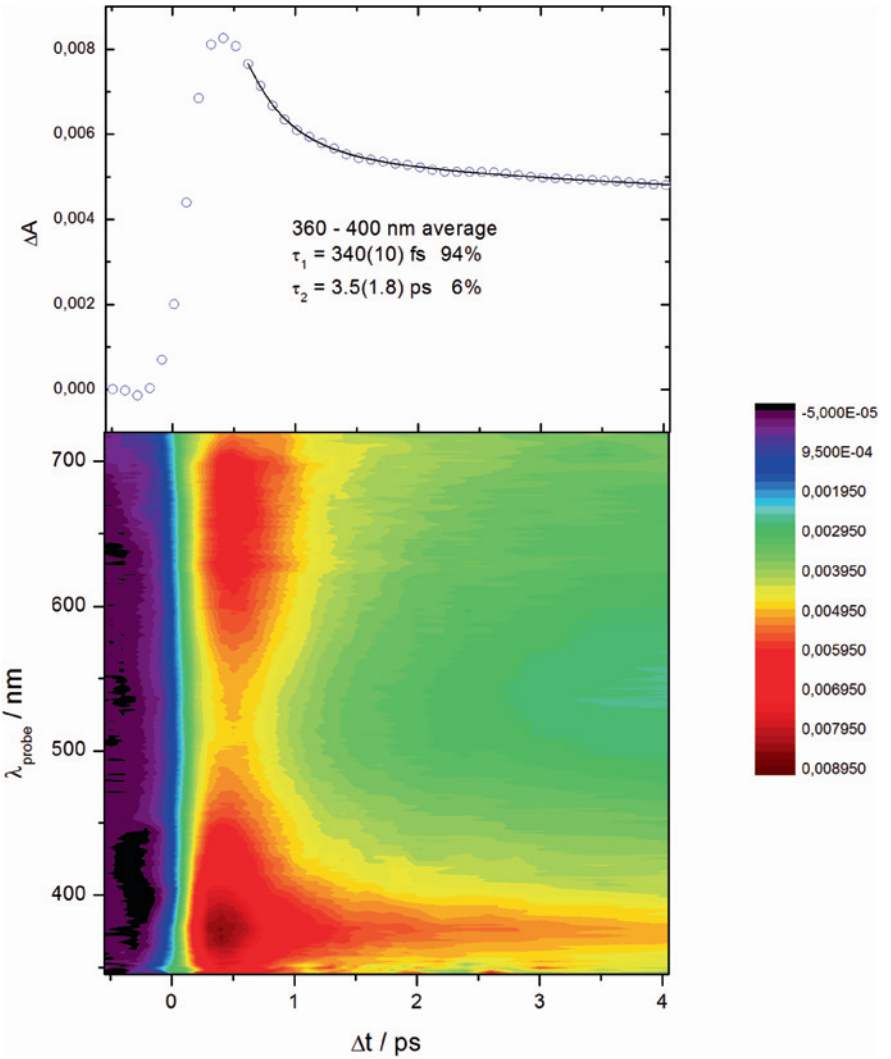


**Figure 11:** Time evolution of transient absorption spectrum of ABPO in $CH_3CN$ after excitation at 258 nm (bottom) and integrated main absorption band between 360 and 400 nm (top).

to form phenyl benzoate after photodissociation of dibenzoyl peroxide [10]. Also, the recombination yield is very different for both reactions: whereas in the case of ABPO ~50% of the initially generated benzoyloxyl radicals react to form the ester (see above) for DBPO only 15%–25% follow this reaction path. Both, the increase in recombination rate and yield can be explained by faster diffusion and less steric hindrance for the reaction of methyl with benzoyloxyl radicals.

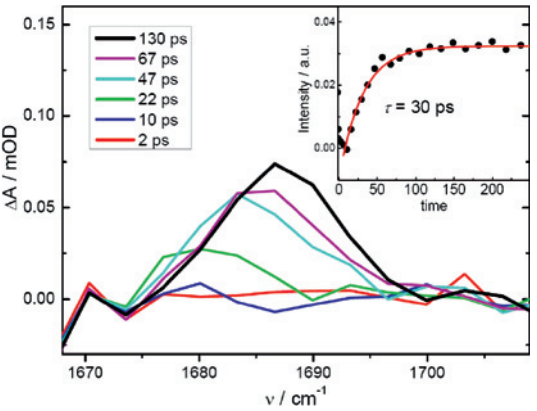


**Figure 12:** Spectral evolution of the C=O stretch absorption band of methyl benzoate formed after photolysis of $A^{13}BPO$ in $CCl_4$. The insert shows the integrated band intensity with an exponential fit (red line).

# 4 Conclusion

We reported results of a femtosecond time resolved study of the ultrafast photofragmentation of acetyl-benzoyl peroxide (ABPO) and 2-naphthoyl-benzoyl peroxide (NBPO) after UV excitation employing $^{13}C$-isotopic labelling of different sites of ABPO and NBPO. For NBPO excitation of the benzoyl part causes decarboxylation exclusively at that site, while after excitation of the naphthoyl moiety apparently about 25% of the energy "leaks" to the benzoyl site. Since electronic excitation transfer from the former to the latter site can be ruled out on energetic grounds, we suggest that rapid IVR is responsible for the observed bond scission at the benzoyl site. The reverse process after excitation of the benzoyl part apparently cannot compete with ultrafast $CO_2$ elimination at that site.

In ABPO the acetyloxyl part completely decarboxylates while only 80%–85% of the benzoyloxyl radicals formed decarboxylate. The remaining radicals either combine with methyl radicals to methyl benzoate within about 30 ps or survive on the time scale of the experiment (1.5 ns). Photofragmentation of ABPO occurs from the $S_1$-state whose lifetime is about 200 fs. All fragments including $CO_2$ appear within the lifetime of electronically excited ABPO. This observation is in line with the fragmentation mechanisms we proposed earlier for other organic peroxides [10, 17, 24].

**Acknowledgement:** We would like to thank Jens Schimpfhauser and Jürgen Bienert who synthesized the compounds needed for this study, and the Deutsche Forschungsgemeinschaft for financial support (SCHR 303/3-1; SCHW 661/3-1).

# References


1. K. Fujimori, Diacyl Peroxides, in: *Organic Peroxides*, W. Ando (Ed.), Wiley, New York (1992), p. 319.
2. J. C. Bevington and T. D. Lewis, T. Faraday Soc. **54** (1958) 1340.
3. J. Chateauneuf, J. Lusztyk, and K. U. Ingold, J. Am. Chem. Soc. **110** (1988) 2886.
4. S. Yamauchi, N. Hirota, S. Takahara, H. Misawa, K. Sawabe, H. Sakuragi, and K. Tokumaru, J. Am. Chem. Soc. **111** (1989) 4402.
5. H. G. Korth, W. Muller, J. Lusztyk, and K. U. Ingold, Angew. Chem. Int. Edit. **28** (1989) 183.
6. A. Kitamura, H. Sakuragi, M. Yoshida, and K. Tokumaru, B. Chem. Soc. Jpn. **53** (1980) 1393.
7. M. Buback, M. Kling, M. T. Seidel, F. D. Schott, J. Schroeder, and U. Steegmüller, Z. Phys. Chem. **215** (2001) 717.
8. B. Abel, J. Assmann, P. Botschwina, M. Buback, M. Kling, R. Oswald, S. Schmatz, J. Schroeder, and T. Witte, J. Phys. Chem. A **107** (2003) 5157.
9. C. Reichardt, T. Schäfer, J. Schroeder, P. Vöhringer, D. Schwarzer, in: *Ultrafast Phenomena XVI*, P. Corkum, S. De Silvestri, K. A. Nelson, E. Riedle, R. W. Schoenlein (Eds.), Springer, Berlin, 2009, pp. 490–492.
10. C. Reichardt, J. Schroeder, P. Vöhringer, and D. Schwarzer, Phys. Chem. Chem. Phys. **10** (2008) 1662.
11. R. Z. Sagdeev, A. A. Obynochny, V. V. Pervukhin, Y. N. Molin, and V. M. Moralyov, Chem. Phys. Lett. **47** (1977) 292.
12. J. M. McBride and M. R. Gisler, Mol. Cryst. Liq. Cryst. **52** (1979) 121.
13. M. Buback, M. Kling, S. Schmatz, and J. Schroeder, Phys. Chem. Chem. Phys. **6** (2004) 5441.
14. J. Pacansky and D. W. Brown, J. Phys. Chem. **87** (1983) 1553.
15. J. Pacansky, G. P. Gardini, and J. Bargon, Ber. Bunsen. Phys. Chem. **82** (1978) 19.
16. J. Pacansky and J. Bargon, J. Am. Chem. Soc. **97** (1975) 6896.
17. C. Reichardt, J. Schroeder, and D. Schwarzer, Phys. Chem. Chem. Phys. **10** (2008) 5218.
18. R. A. Kaindl, M. Wurm, K. Reimann, P. Hamm, A. M. Weiner, and M. Woerner, J. Opt. Soc. Am. B **17** (2000) 2086.
19. P. Hamm and R. A. Kaindl, J. Stenger, Opt. Lett. **25** (2000) 1798.
20. H. Vennekate, A. Walter, D. Fischer, J. Schroeder, and D. Schwarzer, Z. Phys. Chem. **225** (2011) 1089.
21. D. G. Harman, A. Ramachandran, M. Gracanin, and S. J. Blanksby, J. Org. Chem. **71** (2006) 7996.
22. H. Yin, D. L. Hachey, and N. A. Porter, J. Am. Soc. Mass Spectr. **12** (2001) 449.
23. I. P. Zyat'kov, R. Schuster, A. I. Stankevich, and G. A. Pitsevich, Zh. Prikl. Spektrosk. **40** (1984) 230.
24. C. Reichardt, J. Schroeder, and D. Schwarzer, J. Phys. Chem. A **111** (2007) 10111.
25. H. Misawa, K. Sawabe, S. Takahara, H. Sakuragi, and K. Tokumura, Chem. Lett. (1988) 357.